Scientia Iranica B (2016) 23(3), 951–965

SCIENTIA IRANICA

Sharif University of Technology
Scientia Iranica
Transactions B: Mechanical Engineering
www.scientiairanica.com

Effects of uncertainties of conductivity models on mixed convection for Al_2O_3-water nanofluid

A.A. Abbasian Arani* **and R. Dehghani Yazdeli**

Department of Mechanical Engineering, University of Kashan, Kashan, P.O. Box 87317-51167, Iran.

Received 11 November 2013; received in revised form 23 December 2014; accepted 1 August 2015

KEYWORDS
Mixed convection;
Nanofluid;
Variable properties;
Conductivity models;
Uncertainties.

Abstract. The present numerical study aims to investigate the effects of uncertainties of different conductivity models on mixed convection fluid flow and heat transfer in a square cavity filled with Al_2O_3-water nanofluid. The left and right vertical sides of enclosure are maintained at high and low constant temperatures, respectively, while the bottom and top horizontal sides of the enclosure are kept insulated. Furthermore, the right wall moves from down to up with a constant velocity, V_p. To approximate the nanofluid effective thermal conductivity, five most commonly used models, namely, Maxwell, Khanafer and Vafai, Corcione, Chon et al., and Patel et al., are employed. Finite volume method and SIMPLER algorithm are used in order to discretize the governing equations. Simulations are performed for nanoparticles volume fraction ranging from 0 to 0.05 and Richardson number ranging between 0.01 and 100. The results indicate that there are significant differences between the average Nusselt numbers predicted by the five employed conductivity models.

1. Introduction

In engineering and industrial applications such as cooling of electronic equipment, float glass manufacturing, chemical processing equipment, lubrication technologies, and food processing, mixed convection fluid flow and heat transfer are encountered [1-3]. Enhancing the heat transfer rate is one of the essential needs in the above-mentioned applications. In recent years, many researchers have studied the nanofluid, having higher thermal conductivity than the conventional fluids such as water and oil, as an innovative technique to increase the heat transfer rate. Nanofluids are suspensions obtained by dispersing the particles in order of nanometer into the ordinary fluids such as water, oil, and ethylene glycol. Considering nanofluid as the working fluid, many researchers have conducted numerous numerical studies in order to investigate the problem of mixed convection flow and heat transfer inside the rectangular and square cavities.

It should be noted that many of the earlier studies available in the literature [4-12] rely on the Maxwell model [13] and Brinkman model [14] in order to calculate the effective thermal conductivity and viscosity of nanofluid, respectively. While, these models do not take into account the dependency of thermal conductivity and viscosity of the nanofluids on temperature and nanoparticles diameter size. Therefore, the effects of temperature and nanoparticles diameter size on the fluid flow and heat transfer characteristics are not considered. Owing to this defect, some researchers have studied the properties of nanofluid as a function of temperature and nanoparticles diameter size. For instance, Nguyen et al. [15] experimentally investigated the effects of the nanoparticles size and temperature on the viscosity of Al_2O_3-water and CuO-water nanofluids. Using the experimental data reported by Nguyen et al. [15], Abu-Nada et al. [16] derived a correlation in order to calculate the viscosity of

*. *Corresponding author. Tel.: +98 3155912413; Fax: +98 3155912424*
E-mail address: abbasian@kashanu.ac.ir (A.A. Abbasian Arani)

Al_2O_3-water nanofluid as a function of temperature as well as nanoparticles volume fraction. Furthermore, Chon et al. [17] conducted an experimental study and presented a correlation as a function of nanoparticle diameter size, temperature, as well as the nanoparticles volume fraction to predict the thermal conductivity of nanofluids. Besides, Khanafer and Vafai [18] proposed new models, based on the data available in the literature, in order to calculate the thermophysical properties of Al_2O_3-water nanofluid. Their proposed thermal conductivity and viscosity models were as functions of temperature, nanoparticles diameter size, and nanoparticles volume fractions. Corcione [19] also investigated the effects of different parameters on the properties of nanofluids and introduced two empirical correlations to predict the effective thermal conductivity and dynamic viscosity of various nanofluids. In addition to the above authors, Patel et al. [20] presented a correlation in order to calculate the effective thermal conductivity. Recently, aside from the above investigation, there has been some theoretical research emerged to model the nanofluid properties. One of the models is based on this reality that the theoretical models are in conflict with the experimental observations and underpredict the nanofluid heat transfer coefficient. Buongiorno [21] developed an alternative model based on an idea that the anomalous heat transfer occurs due to seven types of slip mechanism of particle migration in the nanofluid. This model has been used by several researchers [22-24]. A new version of this model [25,26] has been presented and applied to different heat transfer regimes [27-31]. The results indicated that the modified model is suitable for considering the effects of nanoparticle migration in nanofluids. On the other hand, active techniques commonly present a higher augmentation though they need additional power that increases initial capital and operational costs of the system.

Employing the proposed correlations by the mentioned authors, some researchers have studied the mixed convection fluid flow and heat transfer of nanofluids with variable thermal conductivity and viscosity within the enclosures. For example, Talebi et al. [32] conducted a numerical study to investigate mixed convection flow and heat transfer of copper-water nanofluid in a square lid-driven enclosure. They used the Patel et al. model [20] and Brinkman model [14] to calculate the effective thermal conductivity and viscosity of nanofluid, respectively. Their results showed that at a given Reynolds number, the average Nusselt number increases with increase in the nanoparticles volume fractions. Also, as the Reynolds number increases, the effect of nanoparticles volume fraction on the flow pattern and thermal behavior decreases. Sheikhzadeh et al. [33] studied the effects of variable properties of Al_2O_3-water nanofluid on the mixed convection heat transfer characteristics in a lid-driven cavity. They employed the Chon et al. model [17] and Abu-Nada et al. model [16] in order to predict the thermal conductivity and viscosity of nanofluid, respectively, and compared the obtained results with those of the Maxwell model [11] and Brinkman model [14]. They reported that at a constant nanoparticles volume fraction, significant differences exist between the values of average Nusselt number for the various employed effective thermal conductivity and viscosity models. Mazrouei Sebdani et al. [34] conducted a numerical investigation to study the problem of mixed convection fluid flow and heat transfer of Al_2O_3-water nanofluid in a lid-driven enclosure using variable thermal conductivity and viscosity. Employing the Chon et al. model [17] and Abu-Nada et al. model [16] for the effective thermal conductivity and viscosity of nanofluids, respectively, they compared the obtained results with those of the Maxwell model [13] and Brinkman model [14]. They concluded that there are significant differences between the magnitudes of heat transfer enhancement for the two different combinations of models. Recently, Chamkha and Abu-Nada [35] presented a numerical study on the effects of different viscosity models on steady laminar mixed convection flow in single and double lid-driven cavities filled with Al_2O_3-water nanofluid. They used two viscosity models, namely, the Brinkman model and the Pak and Cho correlation, in order to approximate nanofluid viscosities. A parametric study is presented to illustrate and compare the effects of two different nanofluid viscosity models. It is found that significant heat transfer enhancement can be obtained due to the presence of nanoparticles and it is accentuated by increasing the nanoparticles volume fractions for moderate and large Richardson numbers with both models using single- and double-lid cavity. However, for small Richardson number, the Pak and Cho model shows a reduction in the average Nusselt number in the single-lid driven cavity configuration. Pourmamoud et al. [36] presented a numerical study on mixed convection fluid flow and heat transfer inside a cavity filled with nanofluid. They examined the effect of type and used model in their investigation. By using two models for dynamic viscosity and two models for thermal conductivity, they concluded that the model of estimation of referred thermophysical properties can influence the heat transfer enhancement. In another research work by Pourmamoud et al. [37], a numerical study was performed on mixed convection flow and heat transfer inside a double lid-driven cavity for CuO-water nanofluid. Based on the obtained results, the empirical correlation proposed by Nguyen et al. [15] was the most accurate model when the effects of nanoparticle diameter and temperature were considered.

To the best of our knowledge, the models pro-

posed by the authors who were mentioned above have separately been used by various researchers to investigate the mixed convection fluid flow and heat transfer of nanofluids in the enclosures. However, examining the uncertainty of different thermal conductivity models for nanofluids, a numerical study has not been performed yet. Therefore, in this work, the effects of uncertainties of thermal conductivity models on steady laminar mixed convection fluid flow and heat transfer for Al_2O_3-water nanofluid are numerically investigated. For this purpose, five different models, used extensively in numerical simulations available in the literature, namely, Maxwell, Khanafer and Vafai, Corcione, Chon et al., and Patel et al. models, are employed in order to predict the effective thermal conductivity. Furthermore, simulations are carried out for various Richardson numbers and nanoparticles volume fractions.

2. Problem definition

The schematic diagram of the cavity is shown in Figure 1. The height and the width of the enclosure are constant and equal to H. By assuming the length of the enclosure perpendicular to the plane of the figure to be enough long, the present problem is considered to be two-dimensional. The right wall moves in its own plane from down to up with a constant velocity, V_p. The right and left vertical walls of the enclosure are kept at constant temperatures of T_h and T_c, respectively, so that $T_h > T_c$, while the top and bottom horizontal walls of the enclosure are kept insulated. The cavity is filled with Al_2O_3-water nanofluid.

It is presumed that the base fluid and the nanoparticles are in thermal equilibrium, and there is no slip between them. The thermophysical properties of nanoparticles and water are presented in Table 1. The thermophysical properties of the nanofluid are assumed to be constant, except for the density, which

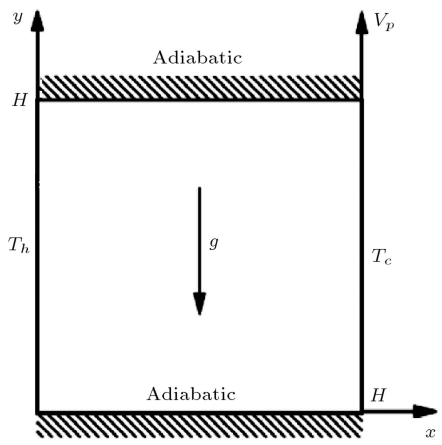

Figure 1. Schematic of the cavity with boundary conditions.

Table 1. Thermophysical properties of water and Al_2O_3 nanoparticles at 25°C [1].

Physical properties	Water	Al_2O_3
c_p (J/kgK)	4179	765
ρ (kg/m^3)	997.1	3970
k (W/mK)	0.613	25
β (K^{-1})	21×10^{-5}	0.85×10^{-5}
d_p (m)	0.384×10^{-9}	47×10^{-9}

is approximated by the Boussinesq model [38]. The nanofluid is considered Newtonian and incompressible. Also the nanofluid flow is presumed to be laminar.

3. Problem formulation

In order to simulate the steady laminar mixed convection flow and heat transfer inside a lid-driven square cavity filled with Al_2O_3-water nanofluid, the finite volume method is used. The governing equations for laminar steady state mixed convection in terms of the two-dimensional steady state continuity, momentum, and energy equations are as follows:

$$\frac{\partial(\rho_{nf}u)}{\partial x} + \frac{\partial(\rho_{nf}v)}{\partial y} = 0, \tag{1}$$

$$\frac{\partial}{\partial x}(\rho_{nf}uu) + \frac{\partial}{\partial y}(\rho_{nf}uv) = -\frac{\partial p}{\partial x} + \frac{\partial}{\partial x}\left(\mu_{nf}\frac{\partial u}{\partial x}\right) + \frac{\partial}{\partial y}\left(\mu_{nf}\frac{\partial u}{\partial y}\right), \tag{2}$$

$$\frac{\partial}{\partial x}(\rho_{nf}vu) + \frac{\partial}{\partial y}(\rho_{nf}vv) = -\frac{\partial p}{\partial y} + \frac{\partial}{\partial x}\left(\mu_{nf}\frac{\partial v}{\partial x}\right) + \frac{\partial}{\partial y}\left(\mu_{nf}\frac{\partial v}{\partial y}\right) + g\rho_{nf}\beta_{nf}(T - T_c), \tag{3}$$

$$\frac{\partial}{\partial x}(\rho_{nf}c_{pnf}uT) + \frac{\partial}{\partial y}(\rho_{nf}c_{pnf}vT) = \frac{\partial}{\partial x}\left(k_{nf}\frac{\partial T}{\partial x}\right) + \frac{\partial}{\partial y}\left(k_{nf}\frac{\partial T}{\partial y}\right). \tag{4}$$

It is worth to say that the initial form of y-momentum equation for the boundary layer is as follows:

$$\frac{\partial}{\partial x}(\rho_{nf}vu) + \frac{\partial}{\partial y}(\rho_{nf}vv) = -\frac{\partial p}{\partial y} + \frac{\partial}{\partial x}\left(\mu_{nf}\frac{\partial v}{\partial x}\right) + \frac{\partial}{\partial y}\left(\mu_{nf}\frac{\partial v}{\partial y}\right) + Y. \tag{5}$$

In the above equation, Y is body force. If the only contribution to this force is made by gravity, the body

force per unit volume is:

$$Y = -\rho_{nf} g, \tag{6}$$

where g is the local acceleration due to gravity. Then, the appropriate form of the y-momentum equation is:

$$\frac{\partial}{\partial x}(\rho_{nf} vu) + \frac{\partial}{\partial y}(\rho_{nf} vv) = -\frac{\partial p}{\partial y} + \frac{\partial}{\partial x}\left(\mu_{nf}\frac{\partial v}{\partial x}\right) + \frac{\partial}{\partial y}\left(\mu_{nf}\frac{\partial v}{\partial y}\right) - \rho_{nf} g, \tag{7}$$

where dp/dy is the free stream pressure gradient in the quiescent region *outside* the boundary layer. In this region, $u = 0$ and the above equation is reduced to:

$$\frac{dp}{dy} = -\rho_{nf\infty} g. \tag{8}$$

Substituting Eq. (4) into (3), we obtain the following expression:

$$\frac{\partial}{\partial x}(\rho_{nf} vu) + \frac{\partial}{\partial y}(\rho_{nf} vv) = \frac{\partial}{\partial x}\left(\mu_{nf}\frac{\partial v}{\partial x}\right) + \frac{\partial}{\partial y}\left(\mu_{nf}\frac{\partial v}{\partial y}\right) + g(\rho_{nf,\infty} - \rho_{nf}). \tag{9}$$

The third term on the right-hand side of Eq. (5) is the buoyancy force per unit mass, and flow is originated by this force because the density is a variable. If density variations are due only to temperature variations, the term may be related to a fluid property known as the *volumetric thermal expansion coefficient*:

$$\beta = -\frac{1}{\rho}\left(\frac{\partial \rho}{\partial T}\right)_p. \tag{10}$$

This *thermodynamic* property of the fluid provides a measure for the amount by which the density changes in response to a change in temperature at constant pressure. If it is expressed in the following approximate form:

$$\beta \approx -\frac{1}{\rho}\left(\frac{(\rho_\infty - \rho)_{nf}}{T_\infty - T}\right), \tag{11}$$

it follows that:

$$(\rho_{nf,\infty} - \rho_{nf}) = \rho_{nf}\beta_{nf}(T_\infty - T). \tag{12}$$

This simplification is known as the *Boussinesq approximation*, and substituting Eq. (12) into Eq. (9), the y-momentum equation becomes:

$$\frac{\partial}{\partial x}(\rho_{nf} vu) + \frac{\partial}{\partial y}(\rho_{nf} vv) = \frac{\partial}{\partial x}\left(\mu_{nf}\frac{\partial v}{\partial x}\right) + \frac{\partial}{\partial y}\left(\mu_{nf}\frac{\partial v}{\partial y}\right) + \rho_{nf}\beta_{nf}(T_\infty - T). \tag{13}$$

For converting the governing equations into dimensionless form, the following dimensionless variables are used:

$$(X, Y) = \frac{(x, y)}{H}, \quad (U, V) = \frac{(u, v)}{V_P}, \quad \theta = \frac{T - T_c}{T_h - T_c},$$

$$P = \frac{p}{\rho_{f,0} V_P^2}, \qquad \mu^* = \frac{\mu_{nf}}{\mu_{f,0}}, \qquad k^* = \frac{k_{nf}}{k_{f,0}},$$

$$\rho^* = \frac{\rho_{nf}}{\rho_{f,0}}, \qquad \beta^* = \frac{\beta_{nf}}{\beta_{f,0}}, \qquad c_p^* = \frac{c_{pnf}}{c_{pf,0}}. \tag{14}$$

After substituting the above variables in Eqs. (1) to (4), the dimensionless form of governing equations are obtained as follows:

$$\frac{\partial(\rho^* U)}{\partial X} + \frac{\partial(\rho^* V)}{\partial Y} = 0, \tag{15}$$

$$\frac{\partial}{\partial X}(\rho^* UU) + \frac{\partial}{\partial Y}(\rho^* UV) = -\frac{\partial P}{\partial X} + \frac{1}{\mathrm{Re}}\left(\frac{\partial}{\partial X}\left(\mu^*\frac{\partial U}{\partial X}\right) + \frac{\partial}{\partial Y}\left(\mu^*\frac{\partial U}{\partial Y}\right)\right), \tag{16}$$

$$\frac{\partial}{\partial X}(\rho^* VU) + \frac{\partial}{\partial Y}(\rho^* VV) = -\frac{\partial P}{\partial Y} + \frac{1}{\mathrm{Re}}\left(\frac{\partial}{\partial X}\left(\mu^*\frac{\partial V}{\partial X}\right) + \frac{\partial}{\partial Y}\left(\mu^*\frac{\partial V}{\partial Y}\right)\right) + \mathrm{Ri}.\theta.\rho^*.\beta^*, \tag{17}$$

$$\frac{\partial}{\partial X}(\rho^* c_p^* U\theta) + \frac{\partial}{\partial Y}(\rho^* c_p^* V\theta) = \frac{1}{\mathrm{Re.Pr}}\left(\frac{\partial}{\partial X}\left(k^*\frac{\partial \theta}{\partial X}\right) + \frac{\partial}{\partial Y}\left(k^*\frac{\partial \theta}{\partial Y}\right)\right), \tag{18}$$

where Reynolds number, Re, Richardson number, Ri, and Prandtl number, Pr, and Grashof number, Gr, are defined as:

$$\mathrm{Re} = \frac{V_P H}{\nu_f}, \qquad \mathrm{Ri} = \frac{g\beta_f(T_h - T_c)H}{V_P^2},$$

$$\mathrm{Pr} = \frac{\nu_f}{\alpha_f}, \qquad \mathrm{Gr} = \frac{g\beta_f(T_h - T_c)H^3}{\nu_f^2}. \tag{19}$$

The boundary conditions are given as:

$$U = 0, \quad V = 0, \quad \theta = 1 \qquad \text{at} \quad X = 0, \tag{20}$$

$$U = 0, \quad V = 1, \quad \theta = 0 \qquad \text{at} \quad X = 1, \tag{21}$$

$$U = 0, \quad V = 0, \quad \frac{\partial \theta}{\partial Y} = 0 \qquad \text{at} \quad Y = 0, \tag{22}$$

$$U = 0, \quad V = 0, \quad \frac{\partial \theta}{\partial Y} = 0 \qquad \text{at} \quad Y = 1. \tag{23}$$

4. Thermophysical properties of the nanofluid

The effective thermophysical properties of the nanofluid can be obtained from various models available in the literature. In the present investigation, the emphasis is on the effects of uncertainties of different thermal conductivity models, which have been extensively used in the studies available in the literature on the mixed convection heat transfer within the cavity. For this purpose, five different conductivity models for the Al_2O_3-water nanofluid, namely, Maxwell, Khanafer and Vafai, Corcione, Chon et al., and Patel et al., are employed.

According to the Maxwell model [13], the effective thermal conductivity of the nanofluid is obtained from the following relation:

$$\frac{k_{nf}}{k_f} = \frac{(k_p + 2k_f) + 2\varphi(k_f - k_p)}{(k_p + 2k_f) + \varphi(k_f - k_p)}. \tag{24}$$

The thermal conductivity correlation proposed by Khanafer and Vafai [18], based on the experimental and theoretical results available in literature, is expressed as:

$$\frac{k_{nf}}{k_f} = 0.9843 + 0.398\phi_p^{0.7383}\left(\frac{1}{d_p(nm)}\right)^{0.2246}\left(\frac{\mu_{nf}(T)}{\mu_f(T)}\right)^{0.0235} - 3.9517\frac{\phi_p}{T} + 34.034\frac{\phi_p^2}{T^3} + 32.509\frac{\phi_p}{T^2}, \tag{25}$$

where, in this correlation, $\phi_p = \varphi * 100$ and $\mu_f(T)$ can be expressed as:

$$\mu_f(T) = 2.414 \times 10^{-5} \times 10^{247.8/(T-140)}. \tag{26}$$

Corcione model [19] for thermal conductivity is also used as follows:

$$\frac{k_{nf}}{k_f} = 1 + 4.4\mathrm{Re}^{0.4}\mathrm{Pr}^{0.66}\left(\frac{T}{T_{fr}}\right)^{10}\left(\frac{k_p}{k_f}\right)^{0.03}\phi^{0.66}, \tag{27}$$

where T_{fr} is the freezing point of the base liquid, and Re, Reynolds number, is defined as:

$$\mathrm{Re} = \frac{2\rho_f k_b T}{\pi\mu_f^2 d_p}. \tag{28}$$

In the above correlation, k_b is Boltzmann's constant and is equal to 1.38066×10^{-23} JK^{-1}.

A thermal conductivity model which has been extensively employed by numerous authors is Chon et al. model [17]. This model is given as:

$$\frac{k_{nf}}{k_f} = 1 + 64.7\phi^{0.7640}\left(\frac{d_f}{d_p}\right)^{0.3690}\left(\frac{k_p}{k_f}\right)^{0.7476} \mathrm{Pr}_T^{0.9955}\mathrm{Re}_T^{1.2321}, \tag{29}$$

where Pr_T and Re_T are defined as follows:

$$\mathrm{Pr}_T = \frac{\mu_f}{\rho_f\alpha_f}, \qquad \mathrm{Re}_T = \frac{\rho_f k_b T}{3\pi\mu_f^2 l_f}. \tag{30}$$

In the above correlation, k_b is Boltzmann's constant and l_f is the mean path of fluid particles and is equal to 0.17 nm [17]. Besides, the Patel et al. model [20] has been extensively used by researchers, too. This model is expressed as:

$$\frac{k_{nf}}{k_f} = 1 + \frac{k_p A_p}{k_f A_f} + ck_p\mathrm{Pe}\frac{A_p}{k_f A_f}, \tag{31}$$

where c is constant and given as 25000, as determined by Patel et al. [20]. A_p/A_f and Pe are defined as:

$$\frac{A_p}{A_f} = \frac{d_p}{d_f}\frac{\phi}{(1-\phi)}, \qquad \mathrm{Pe} = \frac{u_p d_p}{\alpha_f}. \tag{32}$$

Also, u_p is the Brownian motion velocity of nanoparticle and is given as follows:

$$u_p = \frac{2k_b T}{\pi\mu_f d_p^2}. \tag{33}$$

In the above correlations, k_f and k_p are the thermal conductivities of the base fluid and the nanoparticles, respectively, and d_p is mean diameter of the nanoparticle.

To predict the effective dynamic viscosity of the nanofluid, the correlation proposed by Abu-Nada et al. [16], based on the experimental data reported by Nguyen et al. [15], is proposed as follows:

$$\mu_{nf}(cp) = \exp\left(3.003 - 0.04203T - 0.5445\varphi + 0.0002553T^2 + 0.0524\varphi^2 - 1.622\varphi^{-1}\right). \tag{34}$$

To calculate the dynamic viscosity of the base fluid (water) as a function of temperature, the following equation is used [16]:

$$\mu_{\mathrm{H_2O}} = \left(1.2723\times T_{rc}^5 - 8.736\times T_{rc}^4 + 33.708\times T_{rc}^3 - 246.6\times T_{rc}^2 + 518.78\times T_{rc} + 1153.9\right)\times 10^{-6}. \tag{35}$$

In the above correlation, $T_{rc} = \log(T_r - 273)$. The density, heat capacity, thermal expansion coefficient, and thermal diffusivity of the nanofluid are calculated from the following equations, respectively:

$$\rho_{nf} = (1-\varphi)\rho_f + \varphi\rho_p, \tag{36}$$

$$(\rho c_p)_{nf} = (1-\varphi)(\rho c_p)_f + \varphi(\rho c_p)_p, \tag{37}$$

$$(\rho\beta)_{nf} = (1-\varphi)(\rho\beta)_f + \varphi(\rho\beta)_p, \tag{38}$$

$$\alpha_{nf} = \frac{k_{nf}}{(\rho c_p)_{nf}}. \tag{39}$$

The heat transfer coefficient is obtained as:

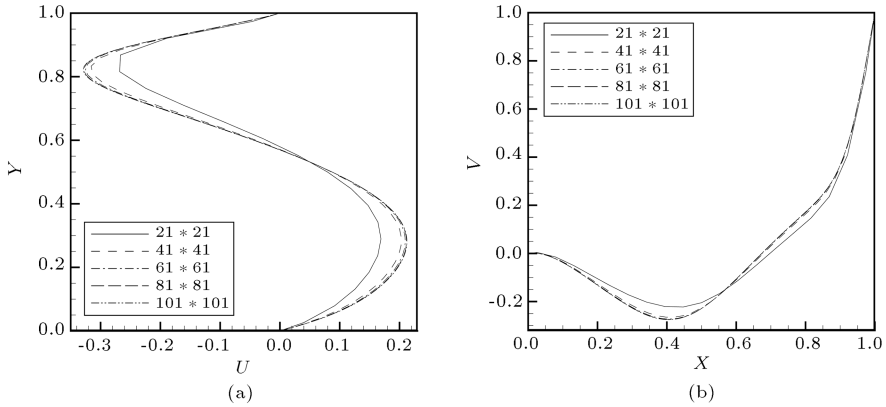

Figure 2. Velocity components along the cavity centerlines for different uniform grids: (a) $U(0.5, Y)$; and (b) $V(X, 0.5)$.

$$h_{nf} = \frac{q''}{T_h - T_c}. \tag{40}$$

The Nusselt number is calculated from the following relation:

$$\mathrm{Nu} = \frac{h_{nf} H}{k_f}. \tag{41}$$

The heat flux of the wall per unit area can be written as:

$$q = k_{nf} \frac{T_h - T_c}{H} \frac{\partial \theta}{\partial X}. \tag{42}$$

By substituting Eqs. (40) and (42) into Eq. (41), the Nusselt number can be obtained as follows:

$$\mathrm{Nu}_{\mathrm{loc}} = \left(\frac{k_{nf}}{k_f} \right) \frac{\partial \theta}{\partial X}. \tag{43}$$

The average Nusselt number along the hot wall is obtained by integrating the local Nusselt number along the left wall as follows:

$$\mathrm{Nu}_{\mathrm{avg}} = \int_0^1 \left(\frac{k_{nf}}{k_f} \right) \frac{\partial \theta}{\partial X} dY. \tag{44}$$

5. Numerical implementation

The finite volume approach is used in order to discretize the governing equations, and for doing the coupling between velocity and pressure fields, the SIMPLER algorithm [39] is applied. The diffusion terms in the equations are discretized using a second order central difference scheme, while a hybrid scheme is employed for approximating the convection terms.

6. Grid independency and validation of the code

In order to determine a grid-independent simulation, five different uniform grids, namely, 21 × 21, 41 × 41, 61 × 61, 81 × 81, and 101 × 101, are employed for simulating the mixed convection heat transfer in the square cavity depicted in Figure 1. The cavity is filled with Al_2O_3-water nanofluid and the calculations are performed for $\mathrm{Ri} = 0.1$, $\varphi = 0.03$, and $\mathrm{Gr} = 10^4$. The results for the X-component of the velocity along the vertical centerline of the cavity, and the Y-component of the velocity along the horizontal centerline of the cavity for these grids are shown in Figure 2(a) and (b), respectively. In addition, variation of Nusselt number versus grid number was presented in Figure 3. Based on the results of Figure 2(a) and (b) and Figure 3, it is realized that a 101 × 101 uniform grid insures the grid-independent solution.

To validate the numerical code, two cases are employed using the presented code, and the results are compared with the results available in the literature. The first case is mixed convection of nanofluid in a lid-driven inclined square cavity with differential heating on top and bottom walls. The obtained results by the

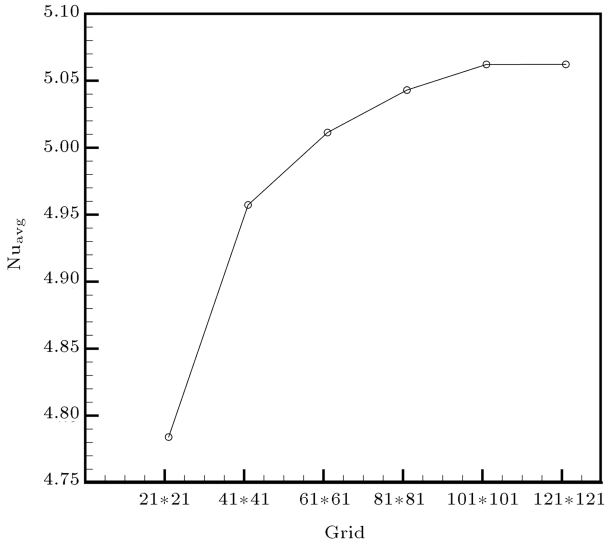

Figure 3. Variations of average Nusselt number on the high constant temperature wall with different uniform grids.

Table 2. Comparison of average Nusselt numbers for the present work and Abu-Nada et al. [5].

	Ri = 0.2	**Ri = 0.5**	**Ri = 2**
Abu-Nada et al. [5]	3.098952	2.554669	1.88441
Present work	3.074891	2.533119	1.89832

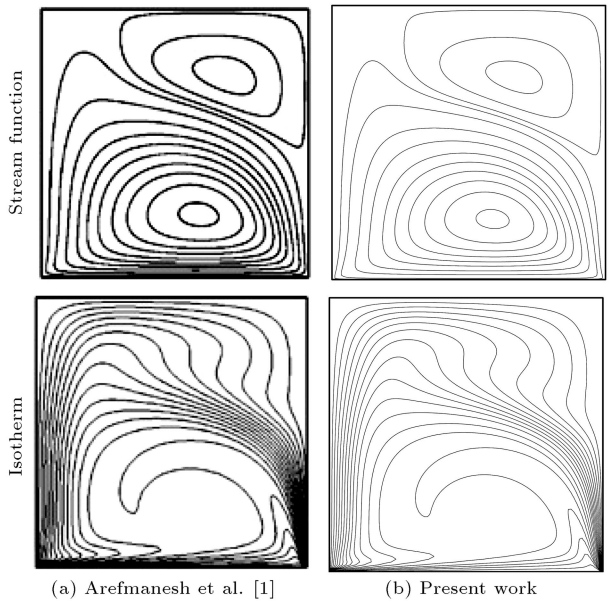

Figure 4. Comparison of stream functions and isotherm contours between the present work and Arefmanesh et al. [1].

present code are compared with those of Abu-Nada et al. [5] in Table 2. These results have been obtained for $\varphi = 0.1$ and inclination angle equal to 0°. As it is noticed from Table 2, there is a good agreement between the present results and those of Abu-Nada et al. [5] for different Richardson numbers.

The second case is mixed convection of nanofluid in a lid-driven square cavity with differential heating on top and bottom walls. The obtained results by the present code are compared with the results of Arefmanesh et al. [1] for $\varphi = 0.03$, Ri = 1, and $Gr = 10^4$ in Figure 4 (similar state with Ref. [1]). As shown in Figure 4, very good agreement exists between the present results and those of Arefmanesh et al. [1].

7. Results and discussion

A numerical study has been carried out in order to investigate the effects of the uncertainty of different thermal conductivity models on the steady laminar mixed convection fluid flow and heat transfer for Al_2O_3-water nanofluid. The Grashof number has been considered to be 10^4 for all of the cases. The Richardson number varies from 0.01 to 100 in order to cover a wide range of Richardson numbers. Also, the nanoparticles volume fraction is considered from 0 to 0.05.

In the current investigation, Grashof number is assumed to be constant. Based on the definition of Richardson number, Ri is changed as the value of Reynolds number is varied. As defined in Eq. (19), at relatively high Richardson numbers, the flow and temperature fields are dominated by the effects of natural convection and at relatively low Richardson numbers, the flow and temperature fields are dominated by the effects of forced convection. As a consequence for high Richardson number, heat transfer takes place predominantly as a result of conduction. At Richardson number equal to unity, the effect of the buoyancy driving forces generated by the temperature difference between the two side walls is equal to the effect of the shear driving force generated by the right moving wall. The buoyancy driving force and shear driving force can act in the same direction or in the opposite direction; and the strength of the recirculation structures can be intensified or decreased, respectively. For low Richardson number, the flow and temperature fields within the cavity are dominated by the forced convection effect. Therefore, a strong recirculation is formed. It is worth to note that the range of Richardson numbers were studied in similar work is as follows: Arefmanesh and Mahmoodi [1] from 0.1 to 100, Abu-Nada and Chamkha [5] from 0.001 to 100, Abu-Nada and Chamkha [35] from 0.0001 to 100, Cho et al. [40] from 0.01 to 1000, and Ghasemi and Aminossadati [12] from 0.01 to 100.

Figures 5 and 6 display typical contour maps for the streamlines and isotherms, respectively, for different Richardson numbers as well as nanoparticles volume fractions. For Richardson number equal to 0.01, the movement of the right lid essentially establishes the flow and generates a large, counterclockwise primary recirculation eddy inside the cavity because of the movement of the nanofluid adjacent to its right wall. As shown in Figure 5, increase in the Richardson number intensifies the effect of the natural convection on the fluid flow and heat transfer inside the cavity when the nanoparticles volume fraction and Grashof number are constant. This manner can be understood by attending to the definition of the Richardson number. The Richardson number is the ratio of buoyancy-driven natural convection to lid-driven forced convection. Hence, for very small values of Richardson number, the forced convection is dominant, so the flow field is mainly established by the movement of the right wall, and the heat transfer occurs primarily through forced convection; and for very high values of that, natural convection is dominant, therefore the heat transfer occurs primarily through natural convection.

As it is clear in Figure 5, at relatively high values of the Richardson number, two different recirculation eddies are developed inside the cavity; one at the left side of the cavity and other at the right side of the

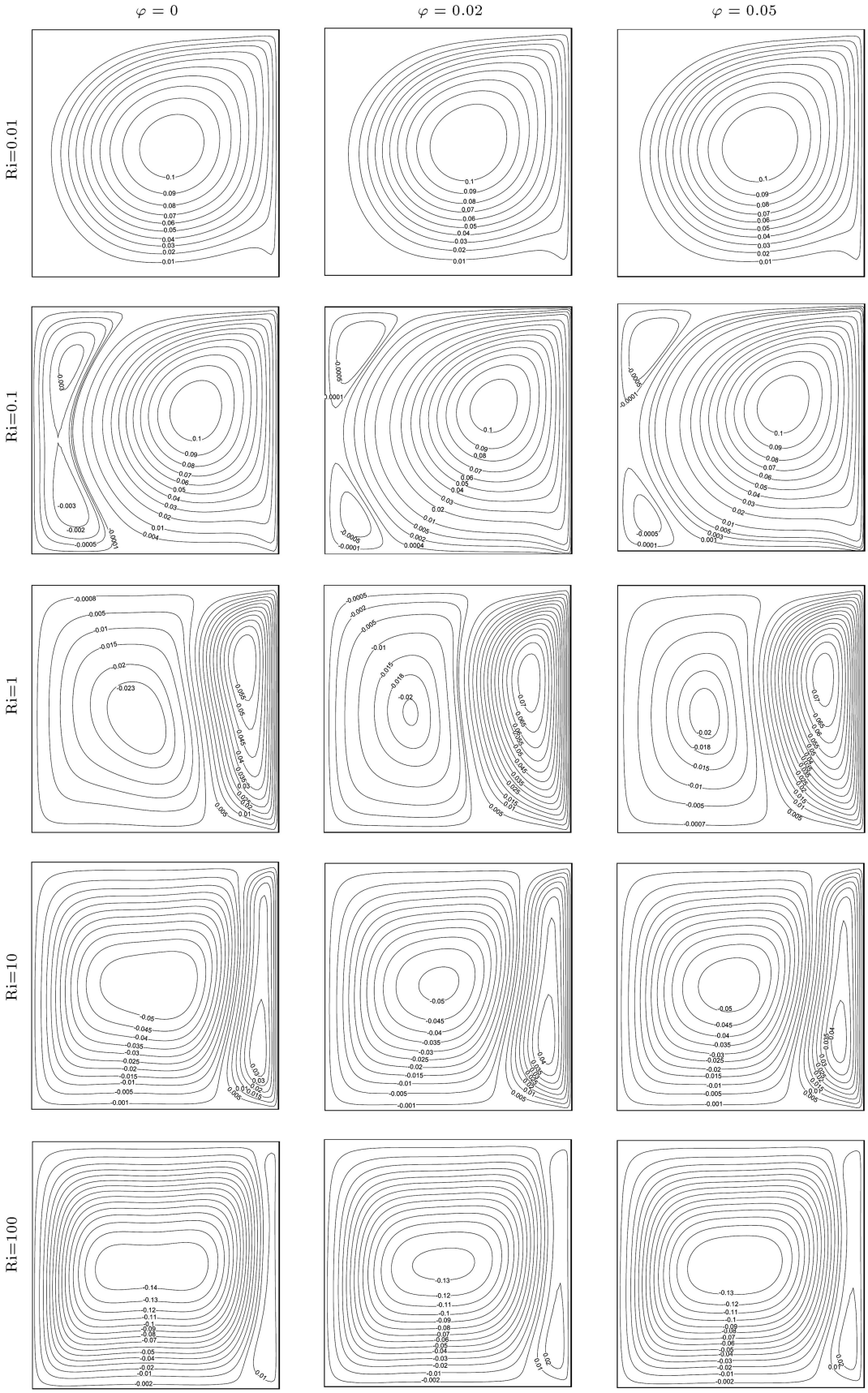

Figure 5. Contours of stream lines for different Richardson numbers and nanoparticles volume fractions using Maxwell model.

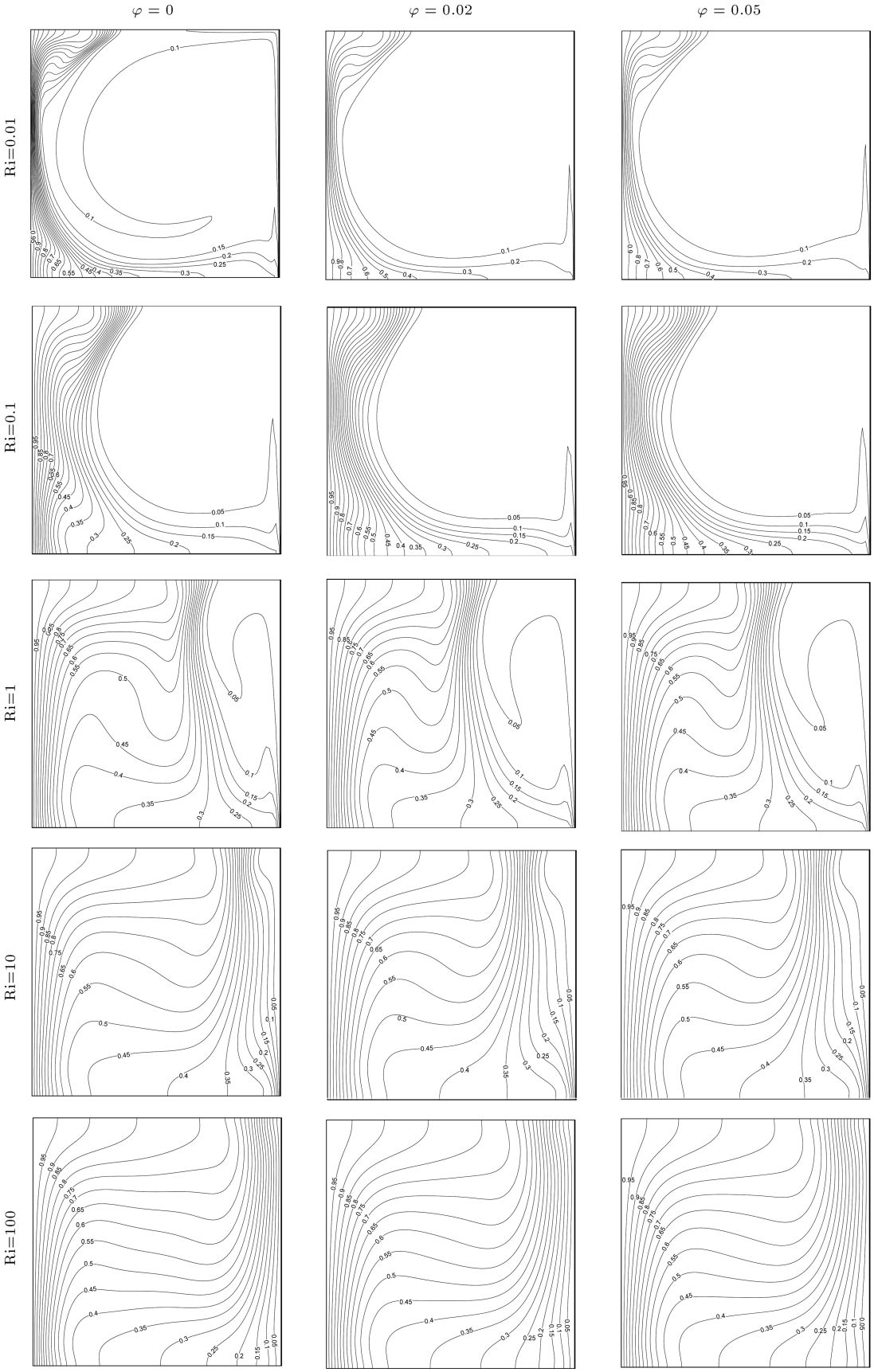

Figure 6. Contours of isotherms for different Richardson numbers and nanoparticles volume fractions using Maxwell model.

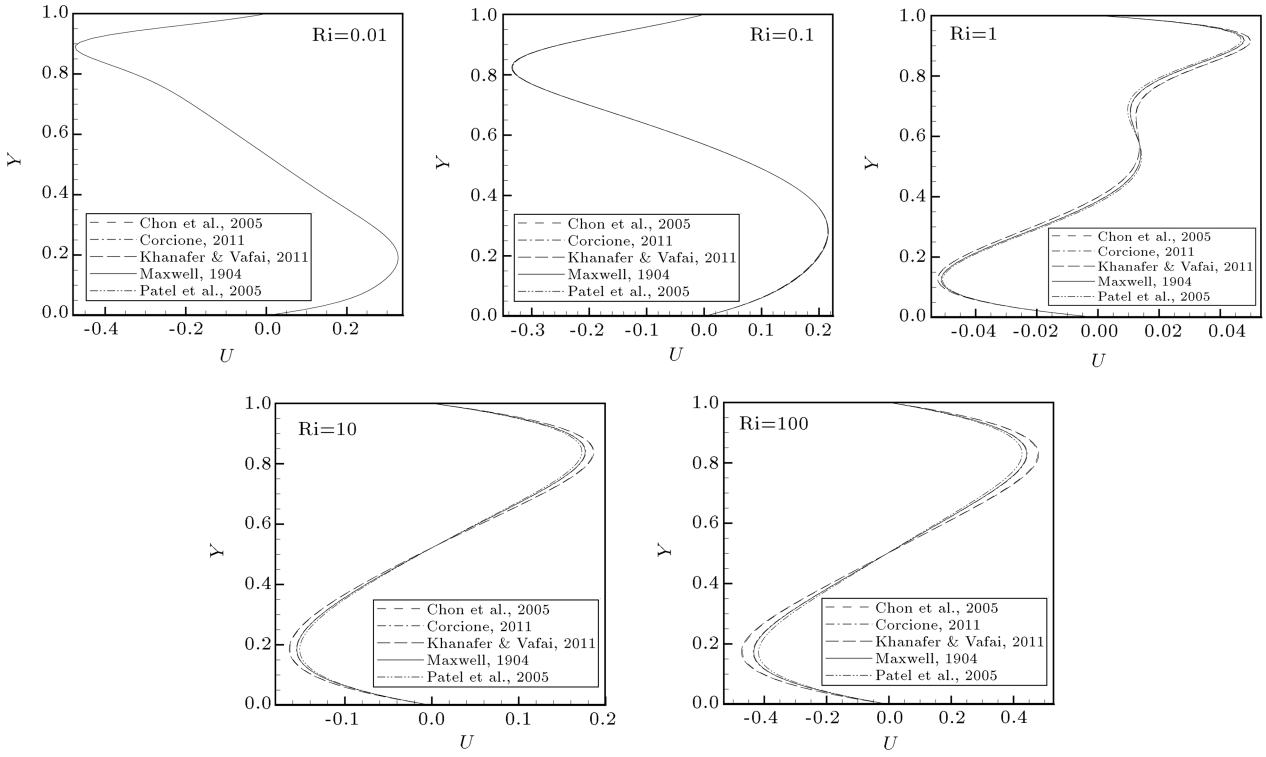

Figure 7. Typical profiles of X-component of velocity U for various Richardson numbers using different thermal conductivity models at $\varphi = 0.03$.

cavity. The eddy at the left side is generated due to the buoyancy-driven natural convection, and the other one is generated due to the lid-driven forced convection. Therefore, for high values of Richardson number, on which the natural convection is dominant, the eddy at the left side is larger and vice versa.

As shown in Figure 6, as the Richardson number increases, the isotherms tend to the isotherms corresponding with the natural convection, in particular, at Richardson number equal to 100, in which the isotherms are the same as those of natural convection fluid flow in an enclosure.

Figures 7 and 8 illustrate variations of the component of the dimensionless horizontal and vertical velocities along the vertical and horizontal centerlines of the cavity, respectively, with Richardson number at nanoparticles volume fraction equal to 0.03 for five employed thermal conductivity models. As shown in Figures 7 and 8, the components of the dimensionless velocity along the vertical and horizontal centerlines of the cavity are affected by different models, especially at high values of Richardson number. Also, the component of the dimensionless horizontal velocity along the vertical centerline is affected more than the vertical velocity along the horizontal centerline. This manner might be interpreted in the way that was discussed above; when the Richardson number has a high value, the regime of flow is basically natural convection. Thus, the increase and decrease of effective thermal conductivity affect the behavior of flow and heat transfer. While, at very low values of the Richardson numbers, the flow regime is basically forced convection and variations of effective thermal conductivity are insignificant.

Figure 9 indicates the average Nusselt numbers of the hot wall of the cavity with respect to the nanoparticles volume fraction for different Richardson numbers using five thermal conductivity models. As shown in Figure 9, for all of the five used thermal conductivity models, with increase in the nanoparticles volume fraction, average Nusselt number first increases to $\varphi = 0.01$, then it decreases to $\varphi = 0.02$, and it continuously increases to $\varphi = 0.05$ at all Richardson numbers except Ri = 0.1. At Ri = 0.1, for all the five used thermal conductivity models, as the nanoparticles volume fraction increases, the average Nusselt number increases. Moreover, as it can be observed from Figure 9, the Patel et al. model [20] predicts minimum value for the average Nusselt number of the hot wall than average Nusselt number predicted by other employed thermal conductivity models. Furthermore, both the Corcione and Maxwell models estimate the average Nusselt number with an approximately same trend. This can also be concluded for both Khanafer and Vafai and Chon et al. models.

It is interesting to note that for all Richardson numbers except Ri = 0.1, unlike what has been reported in the earlier numerical studies available in the

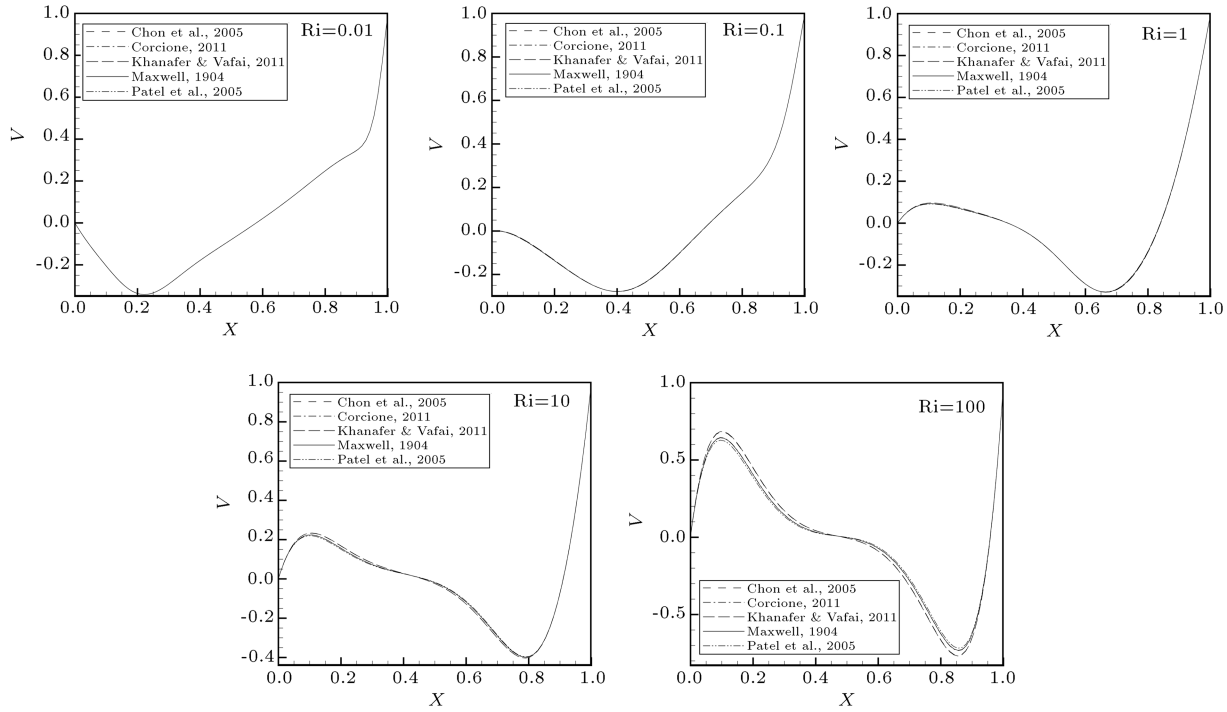

Figure 8. Typical profiles of Y-component of velocity V for various Richardson numbers using different thermal conductivity models at $\varphi = 0.03$.

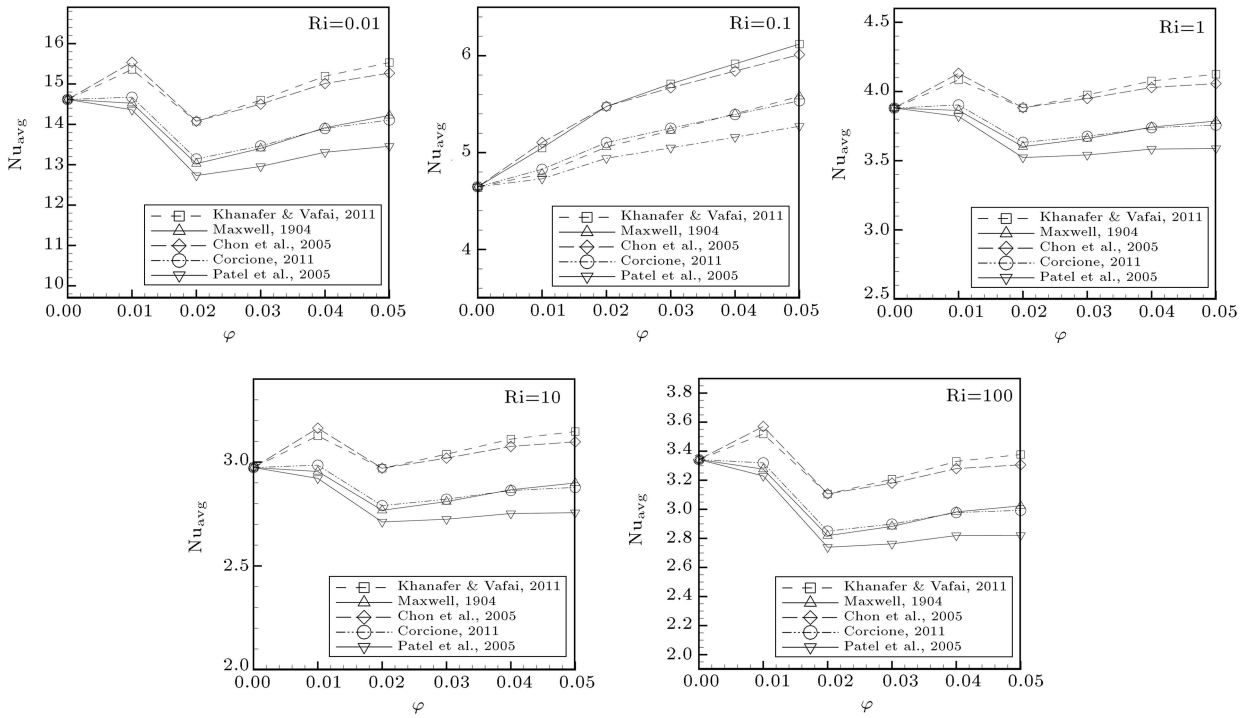

Figure 9. Comparison between average Nusselt numbers obtained using different thermal conductivity models at various Richardson numbers.

literature [12], the average Nusselt number predicted by Maxwell model does not continuously increase with increasing the nanoparticles volume fraction. This behavior may be related to the viscosity model used in this study. As mentioned earlier, to predict the viscosity of the nanofluid as a function of temperature as well as nanoparticles volume fraction, the model proposed by Abu-Nada et al. [16] based on the experimental data of Nguyen et al. [15] was employed in this study. Considering this point, it can be concluded that for

the problem of mixed convection, the effect of thermal conductivity model is less significant than that of the viscosity model.

The reason for changing the Nusselt number is the fact that the nanoparticles presented in the base fluid increase the thermal conductivity and the viscosity of the base fluid at the same time, and increase with increasing the particle concentrations. In fact, the increase in the thermal conductivity leads to an enhancement in the heat transfer coefficient, whereas the increase in the viscosity of the fluid leads to an increase in the boundary layer thickness, which results in a decrease in the heat transfer coefficient [41].

As a result, for the nanoparticles volume fraction studied in this work, the effect of thermal conductivity increment may overcome the effect of the increase in the viscosity or vice versa. These results are the same as the large number of investigations reported in literature, such as [42-44].

Moreover, there are a few investigations that believe that the nanoparticles at higher nanoparticles volume fraction may become combined together, which causes the size to became bigger and leads to a decrease in the heat transfer coefficient. According to this study, the present results are found to be different from those obtained by other researchers, such as Pak and Cho [45]. For numerical investigation, the models that are used for thermal conductivity coefficient and dynamic viscosity estimation can also influence the behavior of nanofluids. As discussed above, generally, it is difficult to explain this difference in behaviors. One can be attributed to several factors, such as particle source, particle size, particle shape, particle preparation, and even solution chemistry (e.g., pH value). Hence, more experimental works and theoretical study are needed to exactly explain heat transfer behavior of nanofluids for applying them in practical applications [41].

Figure 10 shows variation of the ratio of thermal conductivity of nanofluid to that of base fluid with nanoparticles volume fraction for five employed models. As can be observed from Figure 10, the Patel et al. model [20] predicts minimum value for the ratio of nanofluid thermal conductivity to base fluid thermal conductivity. In addition, both the Corcione and Maxwell models, and both the Khanafer and Vafai and Chon et al. models predicted the same value and the same trend for this ratio. The values approximated by the Khanafer and Vafai and Chon et al. models are much higher than the values approximated by three other models.

In the last part of results and discussion section, we present the variations of temperature on vertical high temperature side wall in Figure 11. As can be seen from these figures, the variations of temperature along vertical high temperature side wall, based on the used model, are not significantly different from each other. These differences at high nanoparticle volume fraction and high Richardson number are greater than others. The figure indicates the influence of thermal conductivity model and dynamic viscosity model estimation values on fluid flow and heat transfer. It is difficult to verify the reason of equality or inequality of temperature differences, but the important point in this investigation is the value estimated for non-dimensional heat transfer coefficient, Nusselt number. In fact the important point is the difference between the values of Nusselt number that have been estimated by using each model.

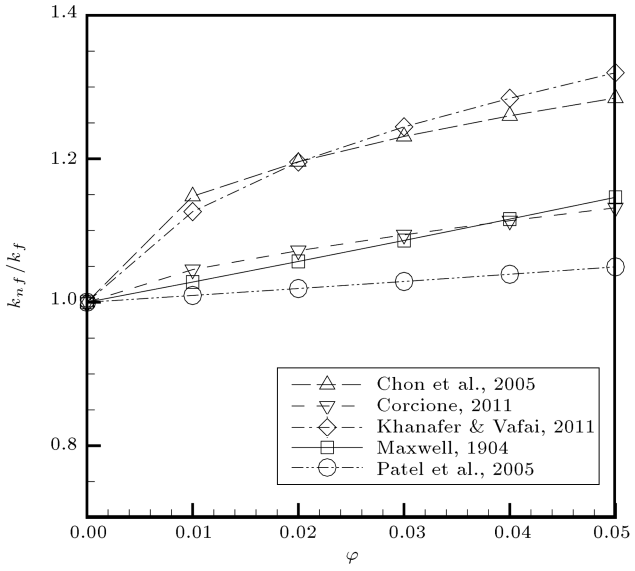

Figure 10. Variation of the ratio of thermal conductivity of nanofluid to that of base fluid with nanoparticles volume fraction for five employed models.

8. Conclusion

In the present study, the problem of steady laminar mixed convection fluid flow and heat transfer of Al_2O_3-water nanofluid in a lid-driven square cavity was numerically investigated. One of the very important points in this study was the variable properties version of governing equations that were used. Another very important point was using the models that were widely used in similar studies. As it is well known, the effect of using nanofluid is not very high; it is very important to clear for the reader that using which model can estimate the enhancement, precisely.

The main focus of this paper was on uncertainties of thermal conductivity models on mixed convection fluid flow and heat transfer characteristic. Therefore, five different thermal conductivity models, namely, Maxwell, Khanafer and Vafai, Corcione, Chon et al., and Patel et al., were employed. The results showed that the heat transfer characteristics within the cavity are strongly dependent on Richardson number as well

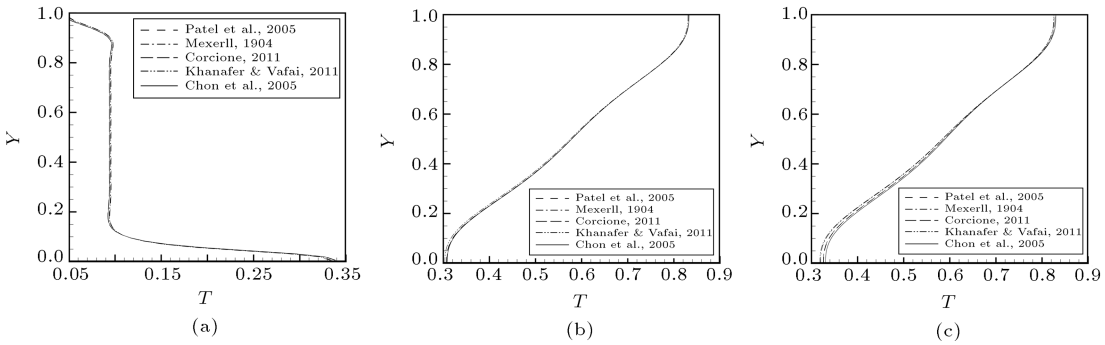

Figure 11. Variations of temperature for different models at (a) Ri = 0.01 and nanoparticles volume fractions of 0.01, (b) Ri = 100 and nanoparticles volume fractions of 0.01, and (c) Ri = 100 and nanoparticles volume fractions of 0.05.

as nanoparticles volume fractions. Based on the obtained results, the following conclusions can be drawn:

- At all Richardson numbers, the predicted average Nusselt number values based on Patel et al. thermal conductivity model [20] were the minimum values in comparison with other employed thermal conductivity models;
- At all Richardson numbers, except Ri = 0.1, for all the five used thermal conductivity models, with increasing the nanoparticles volume fraction, average Nusselt number first increases to $\varphi = 0.01$, then it decreases to $\varphi = 0.02$, and it continuously increases to $\varphi = 0.05$;
- At Ri = 0.1, for all the five used thermal conductivity models, as the nanoparticles volume fraction increases, the average Nusselt number increases;
- For the problem of mixed convection considered in this study, the effect of thermal conductivity model is less significant than that of the viscosity model;
- Using different thermal conductivity models, especially at high values of Richardson number, the component of dimensionless horizontal velocity along the vertical centerline is affected more than the vertical velocity along the horizontal centerline.

Acknowledgment

The authors are appreciative to University of Kashan for supporting this work by Grant No. 55806.

Nomenclature

c_p	Specific heat (J/(kg K))
Gr	Grashof number
d	Diameter of nanoparticles
g	Gravitational acceleration (m/s^2)
h	Heat transfer coefficient (W/(m^{2}K))
k	Thermal conductivity (W/(m K))
k_b	Boltzman constant (J K^{-1}), 1.38066×10^{-23}
H	Enclosure length (m)
Nu	Nusselt number
p	Pressure (N/m^2)
P	Dimensionless pressure
Pr	Prandtl number
Ri	Richardson number
T	Temperature (K)
u, v	Velocity components (m/s)
U, V	Dimensionless velocity components
x, y	Cartesian coordinates (m)
X, Y	Dimensionless Cartesian coordinates

Greek symbols

α	Thermal diffusivity
β	Thermal expansion coefficient
φ	Solid volume fraction
ρ	Density
μ	Dynamic viscosity
ν	Kinematics viscosity
θ	Dimensionless temperature

Subscript

avg	Average
c	Low temperature
f	Fluid
h	High temperature
nf	Nanofluid
p	Particles of solid

References

1. Arefmanesh, A. and Mahmoodi, M. "Effects of uncertainties of viscosity models for Al_2O_3-water nanofluid on mixed convection numerical simulations", *Int. J. Therm. Sci.*, **50**, pp. 1706-1719 (2011).

2. Venkatasubbaiah, K. "The effect of buoyancy on the stability mixed convection flow over a horizontal plate", *European J. Mech. B/Fluids*, **30**(5), pp. 526-533 (2011).
3. Khorasanizadeh, H., Nikfar, M. and Amani, J. "Entropy generation of Cu-water nanofluid mixed convection in a cavity", *European J. Mech. B/Fluids*, **37**, pp. 143-152 (2013).
4. Tiwari, R.K. and Das, M.K. "Heat transfer augmentation in a two-sided lid-driven differentially heated square cavity utilizing nanofluids", *Int. J. Heat Mass Transfer*, **50**, pp. 2002-2018 (2007).
5. Abu-Nada, E. and Chamkha, A.J. "Mixed convection flow in a lid-driven inclined square enclosure filled with a nanofluid", *Eur. J. Mech. B/Fluids*, **29**, pp. 472-482 (2010).
6. Abbasian Arani, A.A., Mazrouei Sebdani, S., Mahmoodi, M., Ardeshiri, A. and Aliakbari, M. "Numerical study of mixed convection flow in a lid-driven cavity with sinusoidal heating on sidewalls using nanofluid", *Superlattices and Microstructures*, **51**, pp. 893-911 (2012).
7. Sivasankaran, S., Sivakumar, V. and Prakash, P. "Numerical study on mixed convection in a lid-driven cavity with non-uniform heating on both sidewalls", *Int. J. Heat Mass Transfer*, **53**, pp. 4304-4315 (2010).
8. Mahmoodi, M. "Mixed convection inside nanofluid filled rectangular enclosures with moving bottom wall", *Therm. Sci.*, **15**, pp. 889-903 (2011).
9. Mansour, M.A., Mohamed, R.A., Abd-Elaziz, M.M. and Ahmed, S.E. "Numerical simulation of mixed convection flows in a square lid-driven cavity partially heated from below using nanofluid", *Int. Commun. Heat Mass Transfer*, **37**, pp. 1504-1512 (2010).
10. Tiwari, R.K. and Das, M.K. "Heat transfer augmentation in two-sided lid-driven differentially heated square cavity utilizing nanofluids", *Int. J. Heat Mass Transfer*, **50**, pp. 2002-2018 (2007).
11. Muthtamilselvan, M., Kandaswamy, P. and Lee, J. "Heat transfer enhancement of copper-water nanofluids in a lid-driven enclosure", *Commun. Nonlinear Sci. Nume. Simu.*, **15**, pp. 1501-1510 (2010).
12. Ghasemi, B. and Aminossadati, S.M. "Mixed convection in a lid-driven triangular enclosure filled with nanofluids", *Int. Commun. Heat Mass Transfer*, **37**, pp. 1142-1148 (2010).
13. Maxwell, J., *A Treatise on Electricity and Magnetism*, Second Ed., Oxford University Press, Cambridge, UK (1904).
14. Brinkman, H.C. "The viscosity of concentrated suspensions and solutions", *J. Chem. Phys.*, **20**, pp. 571-581 (1952).
15. Nguyen, C., Desgranges, F., Roy, G., Galanis, N., Mare, T., Boucher, S. and Anguemintsa, H. "Temperature and particle-size dependent viscosity data for water-based nanofluids-hysteresis phenomenon", *Int. J. Heat Fluid Flow*, **28**(6), pp. 1492-1506 (2007).
16. Abu-Nada, E., Masoud, Z., Oztop, H.F. and Compo, A. "Effect of nanofluid variable properties on natural convection in enclosures", *Int. J. Therm. Sci.*, **49**, pp. 479-491 (2010).
17. Chon, C.H., Kihm, K.D., Lee, S.P. and Choi, S.U.S. "Empirical correlation finding the role of temperature and particle size for nanofluid (Al_2O_3) thermal conductivity enhancement", *Appl. Phys. Lett.*, **87**, p. 153107 (2005).
18. Khanafer, K. and Vafai, K. "A critical synthesis of thermophysical characteristics of nanofluids", *Int. J. Heat Mass Transfer*, **54**, pp. 4410-4428 (2011).
19. Corcione, M. "Empirical correlating equations for predicting the effective thermal conductivity and dynamic viscosity of nanofluids", *Energy Conversion and Management*, **52**, pp. 789-793 (2011).
20. Patel, H.E., Pradeep, T., Sundararajan, T., Dasgupta, A., Dasgupta, N. and Das, S.K. "A microconvection model for thermal conductivity of nanofluid", *Pramana-Journal of Physics*, **65**, pp. 863-869 (2005).
21. Buongiorno, J. "Convective transport in nanofluids", *J. Heat Transfer*, **128**, pp. 240-250 (2006).
22. Garoosi, F., Garoosi, S. and Hooman, K. "Numerical simulation of natural convection and mixed convection of the nanofluid in a square cavity using Buongiorno model", *Powder Technology*, **268**, pp. 279-292 (2014).
23. Garoosi, F., Jahanshaloo, L. and Garoosi, S. "Numerical simulation of mixed convection of the nanofluid in heat exchanger using a Buongiorno model", *Powder Technology*, **269**, pp. 296-311 (2015).
24. Karimipour, A., HosseinNezhad, A., D'Orazio, A., Hemmat Esfe, M., Safaei, M.R. and Shirani, E. "Simulation of copper-water nanofluid in a microchannel in slip flow regime using the lattice Boltzmann method", *European J. Mech. B/Fluids*, **49**(Part A), pp. 89-99 (2015).
25. Yang, C., Li, W. and Nakayama, A. "Convective heat transfer of nanofluids in a concentric annulus", *Int. J. Therm. Sci.*, **71**, pp. 249-257 (2013).
26. Yang, C., Li, W., Sano, Y., Mochizuki, M. and Nakayama, A. "On the anomalous convective heat transfer enhancement in nanofluids: a theoretical answer to the nanofluids controversy", *J. Heat Transfer*, **135**(5), 054504 (9 pages) (2013).
27. Moshizi, S.A., Malvandi, A., Ganji, D.D. and Pop, I. "A two-phase theoretical study of Al_2O_3-water nanofluid flow inside a concentric pipe with heat generation/absorption", *Int. J. Therm. Sci.*, **84**, pp. 347-357 (2014).
28. Hedayati, F., Malvandi, A., Kaffash, M.H. and Ganji, D.D. "Fully developed forced convection of alumina/water nanofluid inside microchannels with asymmetric heating", *Powder Technology*, **269**, pp. 520-531 (2015).
29. Malvandi, A., Moshizi, S.A. and Ganji, D.D. "Effect of magnetic fields on heat convection inside a concentric annulus filled with Al_2O_3-water nanofluid", *Advanced Powder Technology*, **25**(6), pp. 1817-1824 (2014).

30. Malvandi, A. and Ganji, D.D. "Mixed convective heat transfer of water/alumina nanofluid inside a vertical microchannel", *Powder Technology*, **263**, pp. 37-44 (2014).

31. Malvandi, A., Moshizi, S.A., Soltani, E.G. and Ganji, D.D. "Modified Buongiorno's model for fully developed mixed convection flow of nanofluids in a vertical annular pipe", *Computer and Fluids*, **89**, pp. 124-132 (2014).

32. Talebi, F., Mahmoudi, A.H. and Shahi, M. "Numerical study of mixed convection flows in a square lid-driven cavity utilizing nanofluid", *Int. Commun. Heat Mass Transfer*, **37**, pp. 79-90 (2010).

33. Sheikhzadeh, G.A., Ebrahim Qomi, M., Hajialigol, N. and Fattahi, A. "Numerical study of mixed convection flows in a lid-driven enclosure filled with nanofluid using variable properties", *Results in Phys.*, **2**, pp. 5-13 (2012).

34. Mazrouei Sebdani, S., Mahmoodi, M. and Hashemi, S.M. "Effect of nanofluid variable properties on mixed convection in a square cavity", *Int. J. Therm. Sci.*, **52**, pp. 112-126 (2012).

35. Chamkha A.J. and Abu-Nada, E. "Mixed convection flow in single- and double-lid driven square cavities filled with water-Al_2O_3 nanofluid: Effect of viscosity models", *Eur. J. Mech. B/Fluids*, **36**, pp. 82-96 (2012).

36. Pourmahmoud, N., Ghafouri, A. and Mirzaee, I. "Numerical study of mixed convection heat transfer in lid-driven cavity utilizing nanofluid: effect of type and model of nanofluid", http://www.doiserbia.nb.rs/ft.aspx?id=0354-98361300053P

37. Pourmahmoud, N., Ghafouri, A. and Mirzaee, I. "Numerical comparison of viscosity models on mixed convection in double lid-driven cavity utilized CuO-water nanofluid", http://www.doiserbia.nb.rs/ft.aspx?id=0354-98361400048P.

38. Bejan, A., *Convection Heat Transfer*, John Wiley & Sons, Inc., Hoboken, New Jersey, USA (2004).

39. Patankar, S.V., *Numerical Heat Transfer and Fluid Flow*, Hemisphere Publishing Corporation, Taylor and Francis Group, New York (1980).

40. Cho C.C., Chen C.L. and Chen C.K. "Mixed convection heat transfer performance of water-based nanofluids in lid-driven cavity with wavy surfaces", *Int. J. Therm. Sci.*, **68**, pp. 181-190 (2013).

41. Abbasian Arani, A.A. and Amani, J. "Experimental investigation of diameter effect on heat transfer performance and pressure drop of TiO_2-water nanofluid", *Exp. Therm. Fluid Sci.*, **44**, pp. 520-533 (2013).

42. He, Y., Jin, Y., Chen, H., Ding, Y., Cang, D. and Lu, H. "Heat transfer and flow behaviour of aqueous suspensions of TiO_2 nanoparticles (nanofluids) flowing upward through a vertical pipe", *Int. J. Heat Mass Transfer*, **50**(11-12), pp. 2272-2281 (2007).

43. Xuan, Y. and Li, Q. "Investigation on convective heat transfer and flow features of nanofluids", *J. Heat Transfer*, **125** (1), pp. 151-155 (2003).

44. Nguyen, C.T., Roy, G., Gauthier, C. and Galanis, N. "Heat transfer enhancement using Al_2O_3-water nanofluid for an electronic liquid cooling system", *Appl. Therm. Eng.*, **27**(8-9), pp. 1501-1506 (2007).

45. Pak, B.C. and Cho, Y.I. "Hydrodynamic and heat transfer study of dispersed fluids with submicron metallic oxide particles", *Exp. Heat Transfer*, **11**(2), pp. 151-170 (1998).

Biographies

Ali Akbar Abbasian Arani received his BSc and MSc degrees from Sharif University of Technology in Tehran, Iran, in 1991 and 1994, respectively. Then, he received his PhD degree from University of Bordeaux 1 in Bordeaux, France, in 2006. Dr. Ali Akbar Abbasian Arani is currently an Associate Professor at the Mechanical Engineering Department of University of Kashan in Kashan, Iran. His current research interests are fluid mechanics & heat transfer, nanofluids, and energy conversion.

Reza Dehghani Yazdeli received his BSc degree from the Islamic Azad University in Kashan, Iran, in 2011. Then, he received his MSc degree from University of Kashan in Kashan, Iran, in 2013. His research interests are computational fluid dynamics, convection heat transfer, and nanofluid.